WORLD CONFERENCE ON TIMBER ENGINEERING 2025
BRISBANE, AUSTRALIA
Advancing Timber for the Future Built Environment

MEASUREMENT AND NUMERICAL REPRODUCTION OF HEAT AND WATER TRANSFER IN FULL-SCALE WOODEN BEAMS EXPOSED TO FIRE HEATING

Tatsuro SUZUKI[1], Yuji HASEMI[2], Tomoyo HOKIBARA[3], Junichi SUZUKI[4], Mei YAMAMOTO[5]

ABSTRACT: Local temperature and moisture content in wooden full-scale beams with short/long heated area were measured and calculated. The mechanical behavior of wooden buildings during fire should be quantitatively evaluated when spans are increased. In the experiments, moisture content increase were measured, and temperature and moisture content hardly changed in the cross section 600 mm away from the heating boundary. Since the distribution decreased as the temperature and moisture content approached the outside of the furnace in the longitudinal direction and the increase in temperature and moisture content was suppressed in the shorter heating area, it is possible that transfer outside of the heating area suppressed the increase in temperature and moisture content in the heating area. In the calculations, a two-dimensional model was built in the longitudinal and heating directions. The results reproduced the increase in moisture content as in the experiment. However, the distribution in the longitudinal direction in the experiment occurred, whereas the distribution within the heating range in the analysis was nearly constant. The construction and verification of a theory that transfer out of the heating area suppresses the increase in moisture content within the heating area is a future task.

KEYWORDS: Fire heating, Full-scale beam, Water transfer, Mechanical properties, Japanese Cedar

1 – INTRODUCTION

In recent years, wooden buildings have become large-scale not only in Japan but also around the world. In Japan, legal amendent and technological developments are progressing so as to make large-scale wooden building possible. High-rise buildings, large-scale buildings and buildings used by an unspecified number of people are being converted to wooden building. Therefore, predicting the fire-resistance performance of wooden members is becoming more important for improving fire safety and designing appropriate size of wooden members.

As wooden buildings become larger, beam spans are also become longer. Increased demand for uses such as classrooms or large area offices will require designing with longer spans. On the other hand, fire resistance performance of wooden members are evaluated with experiment in fire-resistant furnaces of standard prevalent sizes and specifications. Consequently, it is necessary to verify whether fire-resistant performance of members with longer spans can be properly evaluated with the results of experiments in standard fire-resistant furnaces.

In addition, it has recently been reported that moisture content has a significant infuluence on mechanical properties at high temperatures. Water in wood evaporate, transfer, and recondense due to fire heating, thereby decrease mechanical performance with thermal softening. Because water tends to transfer in the direction of wood fibers, as reported in the Ref.[1][2], differences of spans may affect the amount of recondensed water inside the cross section.

In this study, the short beam in a standard fire-resitant furnace and the long beam in a longer fire-resitant furnace were heated under similar conditions, and the inner temperature and moisture content were measured and compared. In addition, so as to verify the theoretical reproducibility and be able to predict the performance of the longer member, innner temperature and moisture content were numericcally reproduced with heat and water transfer analysis and compare with the experimental results.

[1] Tatsuro Suzuki, Adjunct Researcher, Dept. of Architecture, Waseda University, Tokyo, Japan, tatsuro@suzukikoumuten.com

[2] Yuji Hasemi, Professor Emeritus, Dept. of Architecture, Waseda University, Tokyo, Japan, hasemi@waseda.jp

[3] Tomoyo Hokibara, Assistant Prof., Dept. of Architecture, Waseda University, Tokyo, Japan, hokibara@waseda.jp

[4] Junichi Suzuki, Building Research Institute, Ibaraki, Japan, junichi-szk@kenken.go.jp

[5] Mei Yamamoto, Graduate School of Waseda University, Formerly, Tokyo, Japan, kapro2729@asagi.waseda.jp

https://doi.org/10.52202/080513-0512

2 – METHOD

2.1 EXPERIMENTS

HEATING METHOD

The heating methods of the specimens are shown in Figs. 1 and 2. Two different specimens were heated in a horizontal furnace with the ISO834 standard heating temperature curve. Used horizontal furnace was installed in the Building Research Insutitute in Japan. The length of the heating section can be controlled with dividing furnace wall.

SPECIMENS AND CONDITIONS

Experimental conditions are shown in Table 1. The heated area of specimens M and L were set to 4 and 8 m, respectively. In order to measure the water transfer in the axial and fiber direction, the specimens were extended outward from the heating range by 1 m on both sides.

The cross-section of the specimen is shown in Fig. 3. The locations of the temperature and moisture content measurements along the length direction of specimen M and L are shown in Figs. 1 and 2, respectively.

As shown in Fig. 3, thermocouples and moisture content sensors were installed inside the specimen. The device developed by the authors to back-calculate the moisture content from the electrical resistance measured with electorodos embeded inside the specimen, as reported in [3], was applied. Since the moisture content calculated with electrical resistance, the measurable range is generally 10~30%. The lower limit is due to an increase in electrical resistance, which exceeds the range measurable by the measuring device. The upper limit is determined by the fact that as the moisture content increases, the change in electrical resistance with respect to the change in moisture content becomes smaller, resulting in lower accuracy.

As shown in Figs. 1 and 2, temperature and moisture content were measured at three cross sections, X1, 2, and 3, in both specimens; X1 is intended to measure outside the furnace, X2 near the furnace wall, and X3 inside the furnace, and the axial temperature and moisture content shifts are estimated by comparing these measurements.

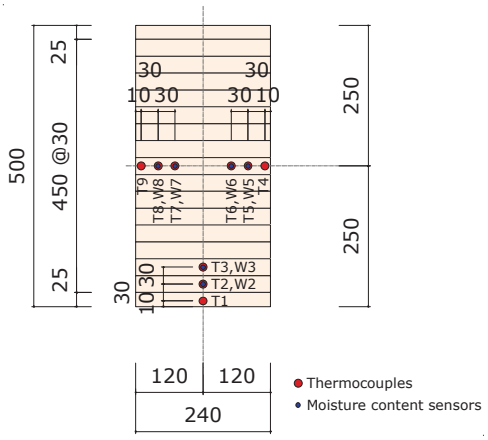

Figure 3 The Cross-section of SpecimenM and L

2.2 CALCULATIONS

OUTLINE

The analysis was performed using the same method as in Ref. [4][5]. In Ref.[4], the basic method of calculating temperature and moisture content moisture with heat and water transfer analysis was reported. In Ref.[5], the temperature and moisture content distribution from heat and water transfer analysis was used to calculate the buckling capacity of the wooden column.

In the analysis, the four main parameters: temperature, moisture content, total pressure, and vapor pressure are calculated in parallel with time. The increase of moisture content is represeted by the evaporation of water near the heated surface, transfer of water vapor to the heated and unheated surfaces, and the recondensation of moisture that has moved to the unheated area.

Table 1 Experimental Condetions

Name	Heated Length [mm]	Length[mm]	Air-dry Density [g/cm^3]	Initial Moisuture Content [%]	Initial Temperature [°C]
M	4,000	6,000	0.32	12.9	24.7
L	8,000	10,000	0.35	13.0	25.7

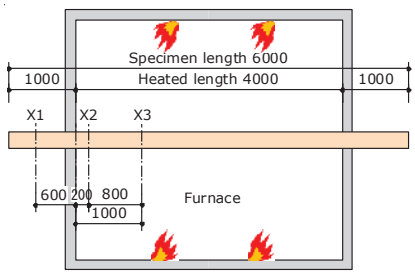

Figure 1 Outline of Specimen M

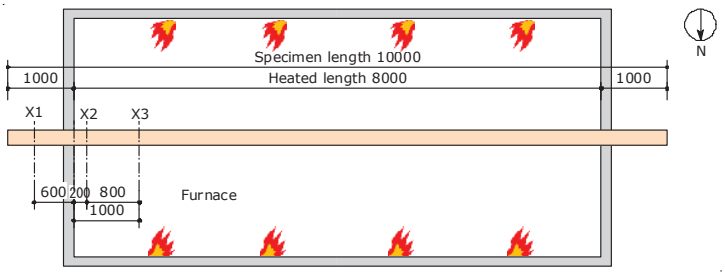

Figure 2 Outline of Specimen L

https://doi.org/10.52202/080513-0512

ALGORITHM

The main formulas from the Ref.[4] are shown below. The basic equations for temperature, moisture content, total pressure, and water vapor pressure are Equations (1) ~ (4). R_{desorp} in equation (2) means the increase or decrease of water content due to the phase change between gas and liquid phases.

(a) Heat transfer

$$\rho_{wood} c \frac{\partial T}{\partial t} = \frac{\partial}{\partial x}\left(\lambda \frac{\partial T}{\partial x}\right) - Q_{desorp} - Q_{evap} - Q_{decomp} + Q_{ox} \quad (1)$$

(b) Water transfer

$$\rho_{wood\ dry} \frac{\partial M}{\partial t} = \frac{\partial}{\partial x}\left(\rho_{wood\ dry} D_w \frac{\partial M}{\partial x}\right) - R_{desorp} - R_{evap} \quad (2)$$

(c) Mixture gas conservation

$$\frac{\partial \varepsilon \rho_g}{\partial t} + \frac{\partial \rho_g u}{\partial x} = R_{desorp} + R_{evap} \quad (3)$$

(d) Vapour conservation

$$\frac{\partial \varepsilon \rho_v}{\partial t} + \frac{\partial \rho_v u}{\partial x} = \frac{\partial}{\partial x}\left(D_v \frac{\partial \rho_v}{\partial x}\right) + R_{desorp} + R_{evap} \quad (4)$$

R_{desorp} is calculated with Equation (5). Equilibrium moisture content M_{eq} was deterimined with temperature and relative humidity. Thus, as the relative humidity increases due to water vapor transfer, the equilibrium moisture content M_{eq} increases, and the adsorption of water vapor increases the moisture content.

In addition, based on mass conservation, if the calculated value of vapor pressure exceeds the saturated water vapor pressure due to the inflow of vapor into each element calculated by Equation (4), the excess is assumed to condense.

$$R_{desorp} = \gamma\,(M - M_{eq}) \quad (5)$$

MODEL

The extent of the modeling of the specimen is shown in Fig. 4 and the model of the analysis is shown in Fig. 5. In this study, a partial area of the specimen was modled in the calculations, and the calculations were performed using long and flat horizontal elements. These are because the simultaneous heat and water transfer analysis is computationally demanding and it was difficult to calculate the entire specimen in three dimensions.

As shown in Fig. 4, cross-sections of the specimen with a width of only 100 mm from the heated surface were modeled. The scope of modeling was limited to 100 mm near the heating surface, where the effects of temperature and moisture content are significant. In reality, there are differences between the bottom and side surfaces of the beam in terms of the direction of the heating, the fibers of the specimen or the presence of adhesive layers; however, these were not considered in the modeling in this study.

As shown in Fig. 5, the specimen was modeled based on an element 10 mm wide and 100 mm long. Considering that heat and water transfer is relatively slower in the direction perpendicular to the heating direction, the calculation load was greatly reduced with increasing the length of the element to 100 mm. Since the specimens are axial symmetrical, half of the length of the specimen was modeled. The model outside the heating range is the same, and the length of the heating range is different, in specimens M and L.

BOUNDARY CONDITIONS

Fig. 5 shows the boundary conditions for each surface. The moisture content was assumed to be adiabatic and similar for all surfaces, assuming no liquid transfer. The top and right sides of the Fig.5 are adiabatic boundaries for temperature, moisture content, total pressure, and vapor pressure, since the specimens are actually continuous.

The lower right of the Fig.5 is the heating range, where the temperature considered radiation and convection, and the total pressure was given by the ambient pressure. The lower left, left side of the figure is the ambient air, and the temperature and total pressure were set to constant values. The vapor pressure on the left, lower side of the figure was assumed to be the outflow multiplied by a factor of the difference in vapor pressure as well as convection.

SETTING PROPERTIES

The parameters used in the analysis are shown in Table 2. Density and moisture content were the average values for specimens M and L. Thermal conductivity of the fiber and longtitudial direction was set to about 1.7 times that of other directions. The permeability in the fiber direction is reported to be extremely large for the radial and perpendicular directions in Ref.[10] and [12], and was set to be 1000 times larger. Heat generation is restricted to 0.4 times the volume to represent the time variation of temperature in the experiment. Consequently, this calculation method has the task of accurate temperature prediction.

The emissivity trends in the longitudinal direction that the 4,8 m specimen receives from the gas mass were estimated from the Ref. [13]. The emissivity near the furnace wall is slightly lower for both M and L.

https://doi.org/10.52202/080513-0512

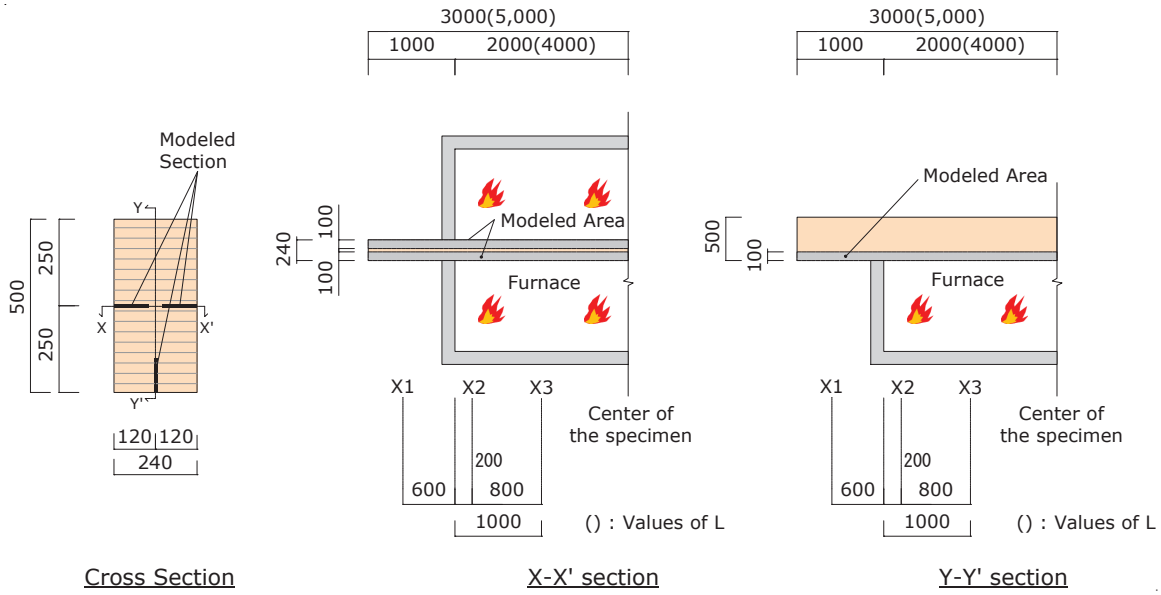

Figure 4 The Extent of the Model in Specimen

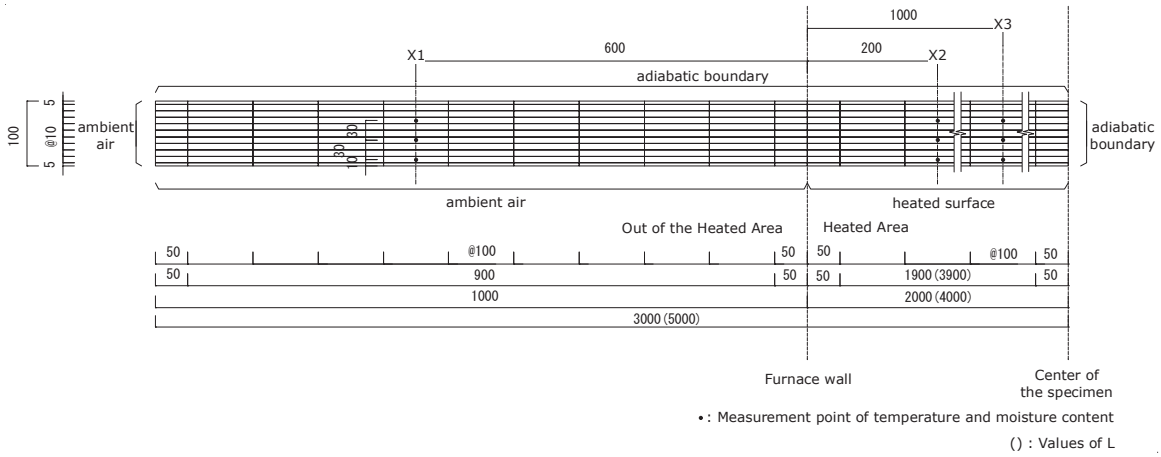

Figure 5 TheModel for Heat and Water Transfer

Table 2 The Properties Setting for Calculations

Symbol	Parameters		Values	Unit
T_{amb}	ambient temperature		20	°C
h_c	convective factor of heat surface		0.04	kW/(m²·K)
ε_r	emissivity of heat surface		0.9	-
h_v	vapor transfer coef.		0.002	kW/(m·K)
T_0	initial temperature		20	°C
U_0	initial relative humidity		0.40	-
$\rho_{wood\,0}$	bone-dry density		300	kg/m³
c_{wood}	heat capacity of	wood	1.236 [6]	kJ/(kg·K)
c_w		water	4.186	kJ/(kg·K)
c_{char}		char	0.883 [7]	kJ/(kg·K)
$\lambda_{R,T}$	thermal conductivity of	radial directions tangential directions	0.832× 10^{-4} [8]	kW/(m·K)
λ_L		longtitudinal directions	1.45× 10^{-4} [8]	kW/(m·K)

Symbol	Parameters		Values	Unit
L_{decomp}	heat of decomposition		3590	kJ/kg
T_{evap1}	evaporation temperature	start	95	°C
T_{evap2}		finish	105	°C
$T_{decomp1}$	decompositon temperature	start	260	°C
$T_{decomp2}$		finish	400	°C
L_w	heat of adsorption and evaporation		2257	kJ/kg
D_w	diffusivity of water		1.94 × 10^{-10} [9]	m²/s
$K_{wood,R,T}$	specific permeability of wood of	radial directions tangential directions	7.11 × 10^{-17} [10]	m²
$K_{wood,L}$		longtitudinal directions	7.11 × 10^{-14}	m²
K_{char}	specific permeability of char		100 K_{wood}	m²
D_{v0}	diffusivity of vapor		3.8 × 10^{-5} [11]	m²/s
γ	rate constant of desorption		0.1	kg/(m³·s)

https://doi.org/10.52202/080513-0512

3 – RESULTS

3.1 EXPERIMENTS

HEATING TEMPERATURE

The heating temperatures inside the furnace are shown in Figs. 6 and 7. In both cases, the average values of the temperatures in furnaces can represent the ISO834 standard heating time temperature curve. In the Ref.[12], differences of heating in the length direction in the furnace used in this study are reported. According to Ref.[12], there is little difference in the incident heat when the specimen is 4,8 m in length that affect the combustion behavior.

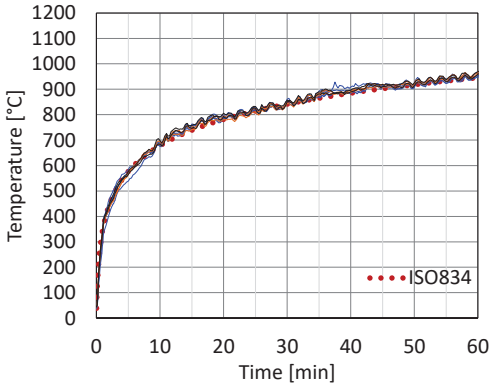

Figure 6 Temperature in the Furnace (Specimen M)

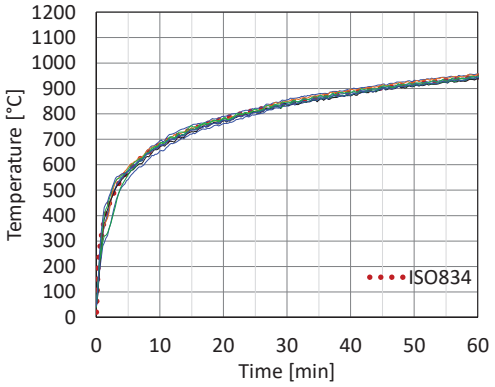

Figure 7 Temperature in the Furnace (Specimen L)

TRANSITION IN EACH CROSS SECTION

Figs. 8, 9, and 10 show the transition of cross sections X1, 2, and 3 of specimen M, and Figs. 11, 12, and 13 show the transition of cross sections X1, 2, and 3 of specimen L, respectively.

For both specimens M and L, the temperature increase at cross section X1 was small and the moisture content changed little. Therefore, the influence of heat and moisture transfer from the heating area was small at cross section transfer from the heating area was small at cross section X1, which is 600 mm away from the heating boundary in the longitudinal direction. However, in both experiments, it was observed that the sealant covered by water vapor swelled at the end of the specimen. Considering these measurement results and observation results, it is considered that there were water that evaporate due to heating, transfer in the fiber and length direction, pass through the part of the specimen outside the heating area, and were released at the end.

TRANSITION IN THE LENGTH DIRECTION

The transition of temperature and moisture content in specimen M is shown in Figs. 14 and 15, and the transition of temperature and moisture content in specimen L is shown in Figs. 16 and 17.

The temperatures of specimens M and L are compared. In the cross section X1, there are almost no differences in the temperature increasing, almost unchanged from room temperature.On the other hand, in the cross sections X2 and X3, the temperature of specimen L is higher, as shown in Fig. and Fig. Because Ref. reported that there is no significant difference between specimens M and L in furnace heating characteristics, the longer heating area may affect the temperature increasing.

Moisture content is compared. There are the errors in the initial moisture content, however; the relative change in moisture content inside the full-scale member can be measured. As well as the temperature, there are little differences in the moisture content increasing in the cross section X1, which is almost unchanged from the initial moisture content. On the other hand, in the cross section X2 and X3, the relative increase tends to be greater for specimen L. For example, At the depth of 70 mm from the heated surface, in the cross section X2, moisture content increased relatively by 2.1% for specimen M and 2.8% for specimen L. In the cross section X3, moisture content increased relatively by 7.0% for specimen M and 13.5% for specimen L Therefore, it is considered that the longer heating range affects not only the temperature but also the moisture content increase.

The reason for the higher temperature and moisture content in specimen L may be that the longer heating area may have resulted in relatively smaller heat and vapor transfer out of the heating area. In the experimental results in Ref.[14], 4 and 8 m beams loaded and heated under the same conditions, both beam was collapsed at the same time even though the charing rate of 4m beam was faster. A possible factor is that the longer span may have affected the increase in internal and moisture content.

3.2 CALCULATIONS

INFLUENCE OF SPECIMEN LENGTH

Figs. 14, 15, and 16 show the transition of cross sections X1, 2, and 3 of specimen M, and Figs. 17, 18, and 19 show the transition of cross sections X1, 2, and 3 of specimen L, respectively.

https://doi.org/10.52202/080513-0512

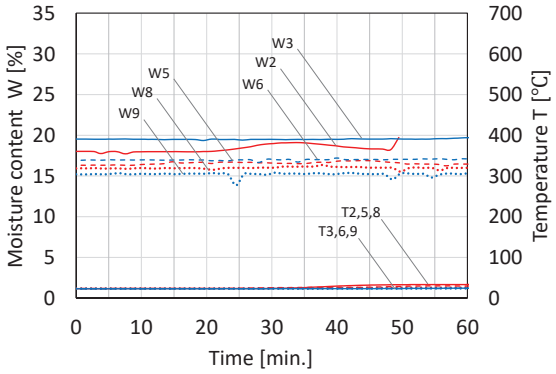

Figure 8 Measurement Result (X1, Specimen M)

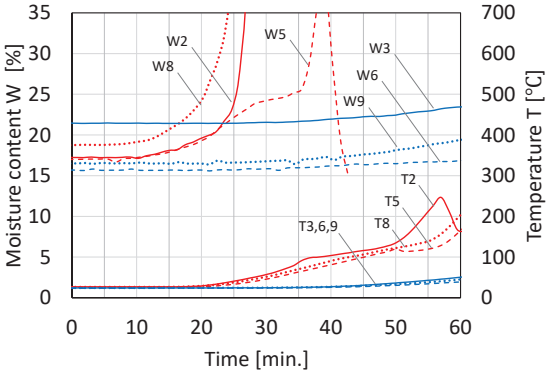

Figure 9 Measurement Result (X2, Specimen M)

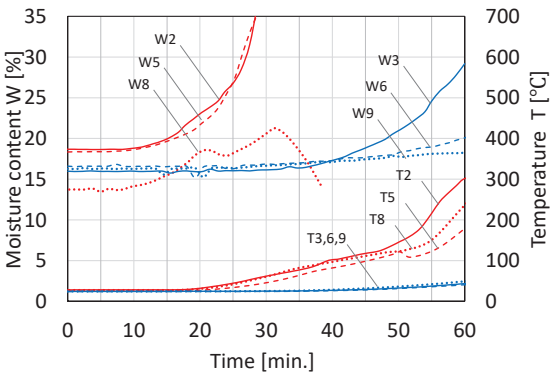

Figure 10 Measurement Result (X3, Specimen M)

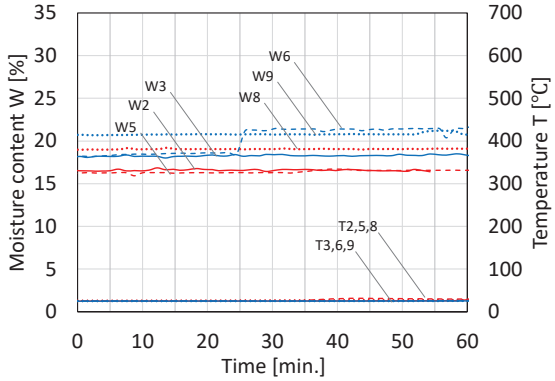

Figure 11 Measurement Result (X1, Specimen L)

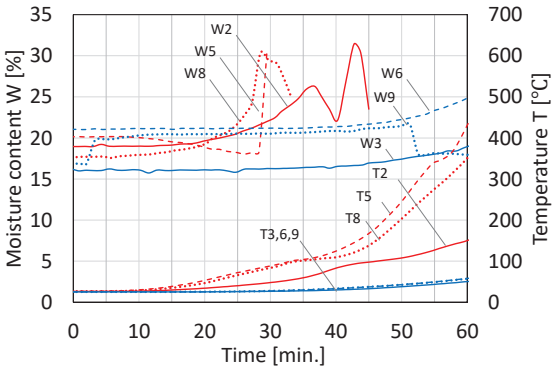

Figure 12 Measurement Result (X2, Specimen L)

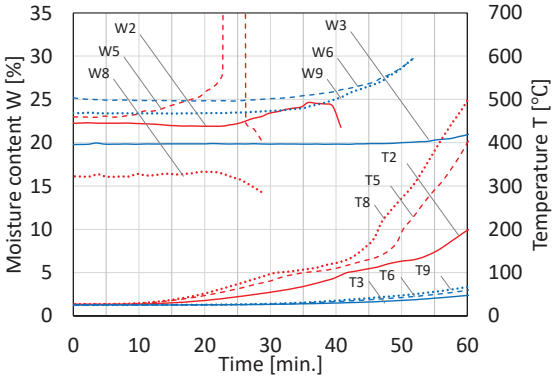

Figure 13 Measurement Result (X3, Specimen L)

Although the temperature of specimen L trended slightly higher, the effect of length on the results of the analysis was insignificant. For example, at cross sections X2 and X3, the temperature at 60 minutes was about 30°C higher for specimen L. On the other hand, the maximum values and transition of moisture content were almost the same for specimens M and L.

TRANSITION IN EACH CROSS SECTION

In cross section X1, the temperature and moisture content remained almost unchanged, with little effect of heating, as in the experimental results. In the analysis, temperature and moisture content increased slightly due to water vapor transfer and adsorption, but remained at 35°C and 3.2%. At the end of the model, the left end of Fig. 5, the moisture content increased to 17.2% at the end of the specimen. The phenomenon of water vapor spouting out from the

https://doi.org/10.52202/080513-0512

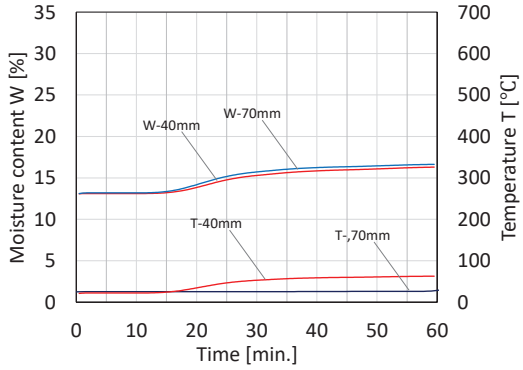

Figure 14 Calculation Result (X1, Specimen M)

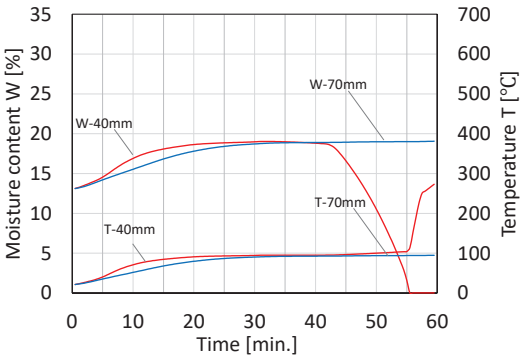

Figure 15 Calculation Result (X2, Specimen M)

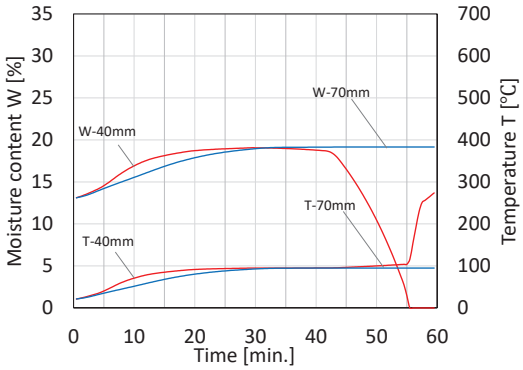

Figure 16 Calculation Result (X3, Specimen M)

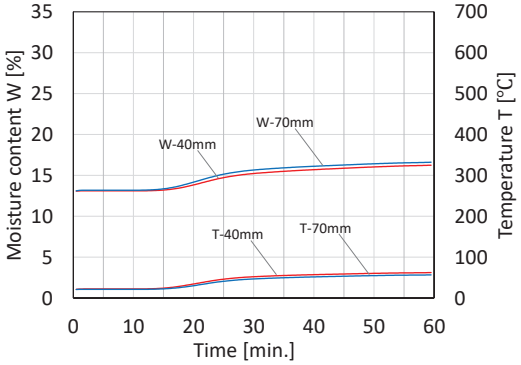

Figure 17 Calculation Result (X1, Specimen L)

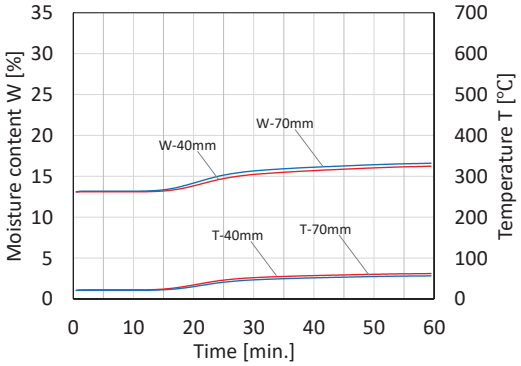

Figure 18 Calculation Result (X2, Specimen L)

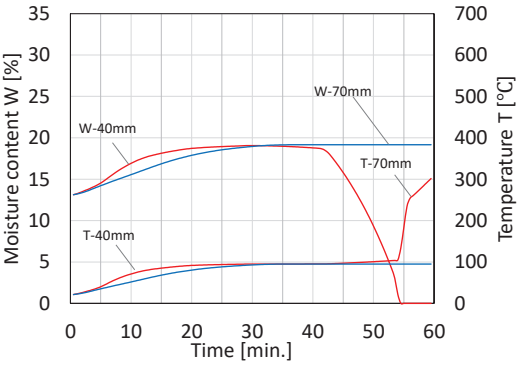

Figure 19 Calculation Result (X3, Specimen L)

end was also confirmed in the experiment, and it is considered to be due to the adsorption of the moving water vapor at the end of the model in the analysis.

TRANSITION IN THE LENGTH DIRECTION

Figs. 20, 21 and 21,22 show the distributions of temperature and moisture content of specimen M and L, respectively.

In the experiment, the temperature and moisture content of cross section X2 migrated lower than that of cross section X3, however; they are almost the same in the analysis. Therefore, it is possible that the analysis may have estimated less heat and moisture transfer outside the heating area of the specimen. As shown in Figs. 20 and 22, the change in temperature near the heating boundary is more gradual in the experiment than in the analysis. As shown in Figs. 21 and 23, the experimental moisture content tends to be higher inside the furnace.

Although the thermal conductivity and permeability were set higher in the fiber and longtitudinal direction, the following additional factors can be mentioned.

https://doi.org/10.52202/080513-0512

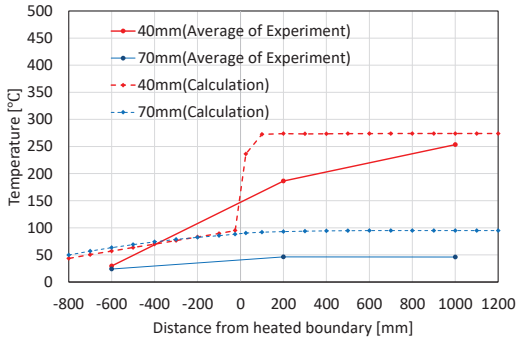

Figure 20 Distribution of temperature(Specimen M and the calculation)

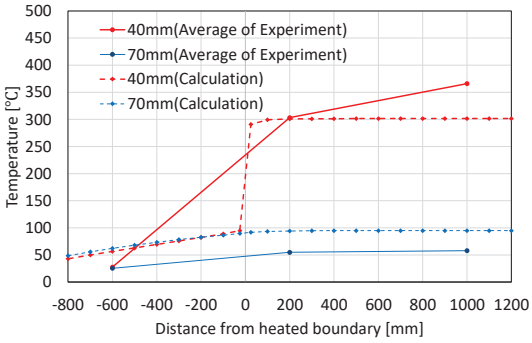

Figure 22 Distribution of temperature(Specimen L and the calculation)

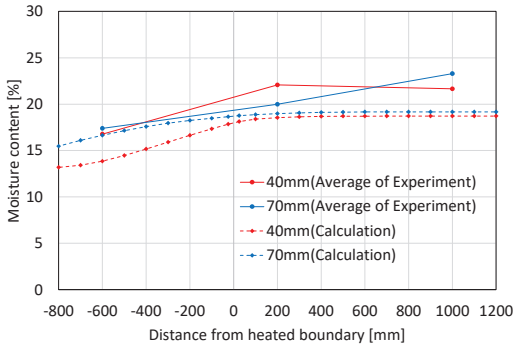

Figure 21 Distribution of Moisture content (Specimen M and the calculation)

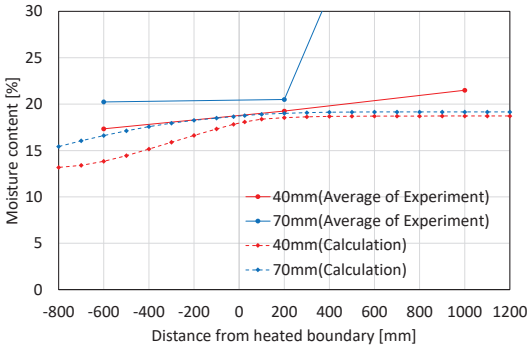

Figure 23 Distribution of Moisture content (Specimen L and the calculation)

In Figs.20-24, red lines show the distributions of 40mm from hated surface at 20 minutes, and blue line show the distributions of 70mm from heated surface at 60 minutes

・The thermal conductivity is further increased by changes in water or temperature.

・The set permeability in the longtitudinal direction was lower than in the experiment. There is an escape route for vapor in the experiment which is not modeled near the heating boundary

・Condensed water vapor moved out of the heating range in liquid phase under the influence of wind velocity and other factors.

・Water vapor is moving out of the heating range through the outside of the modeled area.

Assuming that the temperature and moisture content increasing inside the cross-section in the heating area is suppressed by the water vapor moving outside the heating area, it can be explained that the temperature and moisture content increase in the experiment for specimen L, and that the temperature in cross-section X2 remains lower than that in X3. Although the current analysis shows that the temperatures in the test specimen L remain considerably slightly higher, it is possible that the suppression effect of water vapor moving out of the heating range on the temperature and moisture content increase is calculated lower than in the experiment.

Future work includes the development and verification of a theory that would allow for more active heat and water vapor transfer in the longtitudinal direction.

4 – CONCLUSION

In this study, temperature and moisture content in full-scale beams with short/long heated area, which are exposed to fire heating in unloaded condition, were measured. In addition, a two-dimensional model of a part of the full-scale beam was built, and an analysis was attempted to represent.

HEATING EXPERIMENT

(1) Although the initial moisture content varied, we were able to confirm the phenomenon of moisture content increasing in the full-scale member. In the cross section 600 mm away from the heating boundary, temperature and moisture content hardly changed.

(2) The specimens with a longer heating area showed higher temperatures. In addition, comparing the transitions in the heating area at 200 mm and 1000 mm away from the heating boundary, the temperature

https://doi.org/10.52202/080513-0512

and moisture content remained lower at the 200 mm point closer to the heating boundary. Therefore, it is possible that the increase in temperature and moisture content within the heating area is suppressed by the transfer of heat and water vapor outside the heating area. Furthermore, the suppression effect of temperature and moisture content may become smaller as the span becomes longer.

ANALYSIS AND COMPARISION

(3) Models were built in two dimensions, one in the heating direction and the other in the longitudinal direction of the specimen, allowing for the calculation of temperature and moisture content transitions. Since the length of the specimen overloads the simultaneous heat and water transfer analysis, flat elements with elements lengthened in the longitudinal direction made the calculation possible.

(4) The phenomenon of temperature and moisture content increasing inside the full-scale material could be represented. The longer heating range resulted in slightly higher temperatures, however; the difference in temperature increase due to the difference in the length of the heating area was smaller than in the experiment. In the analysis, the distribution of temperature and moisture content along the length of the heating area was almost constant, and the differences in temperature and moisture content at 200 mm and 1000 mm away from the heating boundary could not be reproduced. Therefore, the analysis could not reproduce almost the effect of the suppression of the temperature and moisture content increase within the heating area due to the transfer of heat and vapor out of the heating area.

Furthermore, the suppression effect of temperature and moisture content may become smaller as the span becomes longer.

Symbols and Greeks

c	heat capacity [kJ/(kg·K)]
D	diffusion coefficient [m^2/s]
E	Young's modulus[N/mm^2]
e_r	emissivity [-]
h_c	convective heat transfer coefficient [kW/(m^2·K)]
h_v	vapour transfer coefficient [m/s]
I	moment of inertia
K	specific permeability [m^2]
L	latent heat [kJ/kg]
L_k	buckling length
M	moisture content [-]
Meq	equilibrium moisture content [-]
M'	molecular weight [kg/kmol]
P	pressure [Pa]
P_k	load
q_{rad}	radiant heat [kW/m^2]
Q	heat generation [kW/m^3]
R	rate of water desorption [kg/(m^3·s)]
T	temperature [°C]
$\bar{T}$	absolute temperature [K]
t	time [s]
u	apparent velocity of gas filtration [m/s]
γ	rate constant of desorption [kg/m^3]
ε	void fraction [-]
κ	Darcy's permeability [m^2/(Pa·s)]
λ	thermal conductivity [W/(m·K)]
ρ	density [kg/m^3]
ρ_{ture}	true density [kg/m^3]

Subscripts

amb	ambient air on heated surface
char	char
decomp	decomposition
desorp	desorption
dry	bone-dry state
evap	evaporation
g	gaseous mixture
max	maximum value
ox	char oxidation
v	vapour
w	water
wood	wood
0	initial
L	longtitudinal directions
R	radial directions
T	tangential directions

5 – REFERENCES

[1] H. Kimura, T. Hokibara, Y. Hasemi, S. Suzuki, T. Suzuki amd R. Takase "Measurement of Directional Characteristics of Moisture Transportation in Wood under Heating" In: World Conference on Timber Engineering, Oslo, Norway, 2023.6. pp.1653-1659

[2] M. Yamamoto, K. Ara, Y. Hasemi, T. Hokibara, R. Takase and T. Suzuki " Measurement of Heat and Water Transfer in the Axial Directioninside Laminated Wood Exposed to Localized Fire (Part 1) Influence of Heated Span on Heat and Water Transfer", pp.153-154, Japan, 2024.7. (in Japanese)

[3] T. Suzuki, Y. Hasemi, D. Kamikawa, N. Yasui and C. Kaku "Developmet of Moisture Content Sensor for Wooden Members Exposed to Fire Heating and Measurement of Moisture Content Distribution during Fire Heating" In: World Conference on Timber Engineering, Santiago, Chile, 2021.8.

[4] T. Suzuki, J. Namiki, Y. Hasemi, R.Takase, D. Kamikawa, N. Yasui, C. Kaku "Measurement of Distribution of Temperature and Moisture Content within Wooden Plate under Steady Heating and Numerical

Reproduction with Heat and Water Transfer Analysis" In: Journal of Environmental Engineering (Transactions of AIJ), Vol.85, No.778, 12.1(2020), pp.891-901, (in Japanese)

[5] T. Suzuki and Y. Hasemi "Calculation Method of Collapse Time of Wood Members Exposed to Fire Heating with Heat and Water Transfer Analysis" In: World Conference on Timber Engineering, Oslo, Norway, 2023.6. pp.1551-1558

[6] Forest Products Laborator "Wood Handbook" Capter 4, pp.4-14, 2021.3.

[7] Forestry and Forest Products Research Institute "Wood Industrials handbook" p834, Maruzen, 1958.12. (in Japanese)

[8] F. Kollman "Technologie des Holzes und der Holzwerkstoffe" In: Springer, Berlin, Heidelberg,1955.8. (in Germany)

[9] T. Yokota "Calculation of Diffusion Coefficient of Moisture Through Cr.miferous Woods" In: Bulletin of the Forestry and Forest Products Research Institute, Vol.173, pp.167-175, 1965.2. (in Japanese)

[10] J. Kawabe and M. Mori "Transverse Air Permeability in Fifteen Wood Species" In: Journal of the Society of Materials Science, The Society of Materials Science, Japan, pp.918-924, 1985.8. (in Japanese)

[11] K. Harada, K. Kajiyama, S. Yusa, S. Uesugi and K. Namiki "Numerical Analysis of Charring Behavior of Wood-based Constructions" In: Summaries of technical papers of AIJ Kinki Chapter research meeting, pp.209-212, 2004.5. (in Japanese)

[12] J. Kawabe and M. Mori "Longtitudinal Air Permeability in Fifteen Wood Species" In: Journal of the Society of Materials Science, The Society of Materials Science, Japan, pp.666-672, 1981.3. (in Japanese)

[13] T. Endo, Y. Hasemi, J. Suzuki, K. Kagiya and T. Hokibara "Examination of Heating Characteristics of Standard Fire Furnace Test for Evaluation of the Mechanical Fire Safety of Beam -Distribution of Incident Heat Flux on Beam during Horizontal Furnace Test and its Dependence on the span length of specimen-" In: Journal of Environmental Engineering (Transactions of AIJ), 88(814):869-880, 2023.12 (in Japanese)

[14] M. Yamamoto, T. Endo, Y. Nakajima, T. Hokibara, Y. Hasemi, J. Suzuki and K. Kagiya " Predictability of the Mechanical Fire Resistance of Long-span Timber Beam Based on Standard Fire Test (Part3) Analysis of the Relationship between Defection/Fracture and Carbonization/Internal Temperature/Incident Heat of the Beams", pp.3074-3077, Japan, 2022.7. (in Japanese)

ACKNOWLEDGEMENTS

The experimtents in this study was supported by the Japan Society for the Promotion of Science (JSPS) Grant Number JP19H00798 (led by Yuji HASEMI).

https://doi.org/10.52202/080513-0512